REPORT DOCUMENTATION PAGE

Form Approved
OMB No. 0704-0188

The public reporting burden for this collection of information is estimated to average 1 hour per response, including the time for reviewing instructions, searching existing data sources, gathering and maintaining the data needed, and completing and reviewing the collection of information. Send comments regarding this burden estimate or any other aspect of this collection of information, including suggestions for reducing the burden, to the Department of Defense, Executive Services and Communications Directorate (0704-0188). Respondents should be aware that notwithstanding any other provision of law, no person shall be subject to any penalty for failing to comply with a collection of information if it does not display a currently valid OMB control number.

PLEASE DO NOT RETURN YOUR FORM TO THE ABOVE ORGANIZATION.

1. REPORT DATE *(DD-MM-YYYY)*	2. REPORT TYPE	3. DATES COVERED *(From - To)*
07-16-2013	Conference Proceedings	

4. TITLE AND SUBTITLE

Measurements of Turbulent Dissipation During the Bahamas Optical Turbulence Experiment

5a. CONTRACT NUMBER

5b. GRANT NUMBER

5c. PROGRAM ELEMENT NUMBER

0601153N

6. AUTHOR(S)

Silvia Matt, Weilin Hou, Sarah Woods, Ewa Jarosz, Wesley Goode and Alan Weidemann

5d. PROJECT NUMBER

5e. TASK NUMBER

5f. WORK UNIT NUMBER

73-6604-03-5

7. PERFORMING ORGANIZATION NAME(S) AND ADDRESS(ES)

Naval Research Laboratory
Oceanography Division
Stennis Space Center, MS 39529-5004

8. PERFORMING ORGANIZATION REPORT NUMBER

NRL/PP/7330--13-1750

9. SPONSORING/MONITORING AGENCY NAME(S) AND ADDRESS(ES)

Office of Naval Research
One Liberty Center
875 North Randolph Street, Suite 1425
Arlington, VA 22203-1995

10. SPONSOR/MONITOR'S ACRONYM(S)

ONR

11. SPONSOR/MONITOR'S REPORT NUMBER(S)

12. DISTRIBUTION/AVAILABILITY STATEMENT

Approved for public release, distribution is unlimited.

13. SUPPLEMENTARY NOTES

14. ABSTRACT

The Bahamas Optical Turbulence Experiment (BOTEX) was conducted in the summer of 2011 to investigate the impact of turbulence on underwater optical imaging. Underwater optical properties can be affected by turbulence in the water, due to localized changes in the index of refraction. We discuss measurements of current velocity and temperature, made with a Nortek Vector Acoustic Doppler Velocimeter (ADV) and PME Conductivity- Temperature (CT) probe, as well as observations made with a Rockland Oceanographic Vertical Microstructure Profiler (VMP). The instruments were deployed in close proximity in the field and in the context of measurements of optical target clarity. Turbulent kinetic energy dissipation (TKED) and temperature dissipation (TD) rates are calculated from the ADV/CT measurements and compared to TKED and TD estimated from the data collected with the VMP. The results show reasonable agreement between the two methods; differences are attributed to turbulence patchiness and intermittence, as well as sampling challenges. The study also highlights the importance of collecting concurrent data on temperature, current velocity, and current shear to assess the turbulence impact on underwater optical properties.

15. SUBJECT TERMS

optical turbulence, TKED, TD, turbulence measurements

16. SECURITY CLASSIFICATION OF:			17. LIMITATION OF ABSTRACT	18. NUMBER OF PAGES	19a. NAME OF RESPONSIBLE PERSON
a. REPORT	b. ABSTRACT	c. THIS PAGE			Weilin Hou
Unclassified	Unclassified	Unclassified	UU	10	19b. TELEPHONE NUMBER *(Include area code)* (228) 688-5257

Reset

Standard Form 298 (Rev. 8/98)
Prescribed by ANSI Std. Z39.18

Measurements of turbulent dissipation during the Bahamas Optical Turbulence Experiment

Silvia Matt [1,2], Weilin Hou [2], Sarah Woods [3], Ewa Jarosz [2], Wesley Goode [2], and Alan Weidemann [2]

[1] National Research Council Postdoctoral Research Associate
[2] Ocean Sciences Branch, Naval Research Laboratory, Stennis Space Center, MS, USA
[3] NRL ASEE Postdoctoral Fellow ‡

ABSTRACT

The Bahamas Optical Turbulence Experiment (BOTEX) was conducted in the summer of 2011 to investigate the impact of turbulence on underwater optical imaging. Underwater optical properties can be affected by turbulence in the water, due to localized changes in the index of refraction. We discuss measurements of current velocity and temperature, made with a Nortek Vector Acoustic Doppler Velocimeter (ADV) and PME Conductivity-Temperature (CT) probe, as well as observations made with a Rockland Oceanographic Vertical Microstructure Profiler (VMP). The instruments were deployed in close proximity in the field and in the context of measurements of optical target clarity. Turbulent kinetic energy dissipation (TKED) and temperature dissipation (TD) rates are calculated from the ADV/CT measurements and compared to TKED and TD estimated from the data collected with the VMP. The results show reasonable agreement between the two methods; differences are attributed to turbulence patchiness and intermittence, as well as sampling challenges. The study also highlights the importance of collecting concurrent data on temperature, current velocity, and current shear to assess the turbulence impact on underwater optical properties.

Keywords: optical turbulence, TKED, TD, turbulence measurements

1. INTRODUCTION

Turbulence is ubiquituous in the world's oceans and riverine environments. The small-scale temperature and salinity variations associated with turbulence can lead to localized changes in the index of refraction and underwater optical properties can be affected. It has been demonstrated that optical turbulence can be a limiting factor in oceanic environments, affecting optical signal transmissions that impact various naval and civilian applications, from diver visibility to active and passive remote sensing.[1] To quantify the scope of the impacts from turbulent flows on optical signal transmission, the Bahamas Optical Turbulence Experiment (BOTEX) was conducted in the summer of 2011 (Fig. 1).[2]

2. METHODS

High-resolution velocity and temperature measurements were obtained with a Nortek Vector Acoustic Doppler Velocimeter (ADV) and PME Conductivity-Temperature (CT) microstructure probe. Data were collected in the context of measurements of optical target clarity. A Vertical Microstructure Profiler (VMP) was deployed to get velocity shear and temperature gradient data (manufactured by Rockland Oceanographic Services Inc., Canada and similar to a profiler described in Ref. 3). The turbulent kinetic energy dissipation (TKED) and temperature dissipation (TD) rates were calculated from the ADV/CT measurements via spectral fitting to Kolmogorov spectra (for velocity) and Batchelor specta (for temperature) and compared to TKED and TD estimates from the VMP.[4]

‡now at SPEC Inc., Boulder, CO, USA
Corresponding author: Silvia Matt: E-mail: silvia.matt.ctr.de@nrlssc.navy.mil

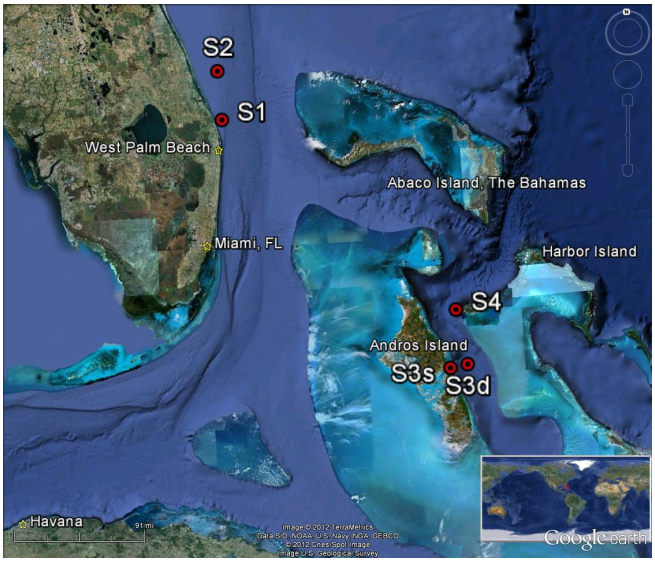

Figure 1. Location of stations during BOTEX.

2.1 Data collection

The ADV and CT probes along with a high-speed imaging camera and optical targets (active and passive; see also Ref. 1) were mounted on a large $5m$ long, rigid aluminum frame termed the Image Measurement Assembly for Subsurface Turbulence (iMast) and were deployed from the ship's A-frame (Fig. 2). The frame was paused at several depths for 10-15 min each, to collect time series of high-resolution velocity and temperature/conductivity for the subsequent estimation of TKED and TD rates. Data were collected at a sampling frequency of $32Hz$. The pauses were taken at depths where optical turbulence associated with strong temperature gradients was expected to be most pronounced, i.e. at the bottom of the mixed layer and on either side of the thermocline. For comparison, additional time series were taken in regions of low temperature variability. The Rockland VMP was deployed falling freely through the water column during profiling, more details can be found in Ref. 1.

2.2 Calculation of TKED and TD

2.2.1 Turbulent Kinetic Energy Dissipation rate - TKED

The estimation of TKED rates from velocity time series collected with ADVs is based on the well-established Inertial Subrange Disspiation Method (IDM) (see, f. ex., Ref. 5) and is based on fitting observed velocity spectra to the theoretical energy spectrum of turbulence described by Kolmogorov (see, f. ex., Ref. 6), which exhibits a $-\frac{5}{3}$ slope in the inertial subrange (ISR). The spectral fitting requires that an ISR is present and well-resolved in the spectra. Deployment strategies thus have to take into account platform motion and instrument configuration, as these can introduce motion that may cause contamination of the ISR of the spectrum. Spectra are calculated from velocity time-series, and Taylor's Frozen Turbulence hypothesis (see, f. ex., Ref. 7), $k = \frac{2\pi f}{U}$, is applied to convert the frequency spectra to wavenumber spectra. Here, k is the wavenumber (in $rad\,m^{-1}$), f is the frequency (in s^{-1}), and U is the mean flow past the sensor (in $m\,s^{-1}$). A wavenumber range respresentative of the spectrum in the ISR is chosen and the TKED rate ϵ is estimated from

$$E_{ii}(k_1) = C\epsilon^{\frac{2}{3}} k_1^{-\frac{5}{3}}, \tag{1}$$

where

$$\int_0^\infty E_{ii}(k_1)\, dk_1 = \bar{u}_i^2. \tag{2}$$

Here, E_{ii} is the one-dimensional velocity spectrum of component i ($x_1 = x$ is the streamwise component, $x_2 = y$ is the transverse component, and $x_3 = z$ is the vertical component, in a Cartesian coordinate system), and

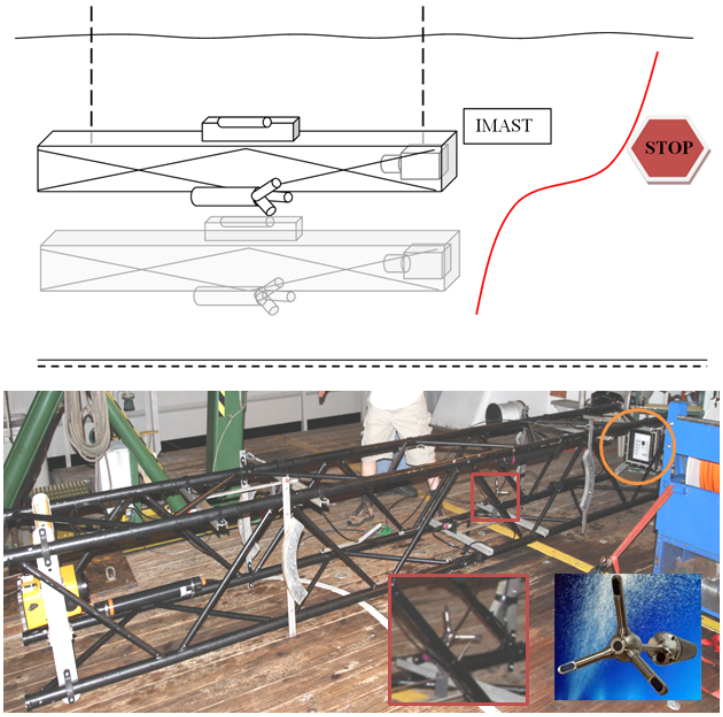

Figure 2. Schematic of iMast deployment during BOTEX (top) and photograph of iMast on deck showing the ADV/CT probes mounted on the frame, the high-speed camera and the iPad as optical target (bottom).

$\bar{u}_i^2$ is the variance of the signal. C is a constant equal to $\frac{18}{55}\,\alpha$ in the streamwise direction (x and k_1) and to $\frac{4}{3}\,\frac{18}{55}\,\alpha$ in the transverse or vertical direction (y, z) ; $\alpha \approx 1.5$ is the Kolmogorov constant.[8] Since a considerable source of uncertainty in the estimation of ϵ is introduced through the choice of the mean flow U for the application of Taylor's Frozen Turbulence hypothesis, we follow Ref. 5 and rotate our observed velocities (which were collected in XYZ-coordinates, the coordinate system of the sensor, then rotated into geophysical coordinates) into a new frame of reference where $\overline{U} = (\overline{U}_1, 0, 0)$.[5] $\overline{U}_1$ is then used in the conversion from frequency to wavenumber space. Resolving the ISR also puts a minimum requirement on the record length, and data segments from the $10 - 15min$ depth pauses were chosen as long as possible, within the constraints of excessively noisy data and directional changes in mean flow U. For our data, the wavenumber range to fit to the theoretical spectrum was chosen manually, we found this to yield a more robust result than automating the routine, especially in the case of noisy spectra. The fit to the data was accomplished by using the approach introduced by Ref. 5, based on a maximum likelihood estimator (MLE) technique, previously used for Batchelor spectral fitting.[9] This approach also allows the estimation of errors on TKED through the MLE method as described in Ref. 5 and Ref. 9.

One issue that arose in our data was the occurence of so-called "phase-wrapping", which can occur if the ambient velocity exceeds the maximum velocity that can be measured by the instrument, the so-called ambiguity velocity. This maximum measureable velocity of the ADV is determined by an instrument setting controlling the pulse separation, the nominal velocity range, and applies to the beam velocities. Phase-wrapping can occur even if the observed earth-referenced velocities do not exceed the estimated maximum velocity range.[10] The phase-wrapping can be corrected for in post-processing. However, the correction has to be applied for the beam velocities and requires a coordinate transformation if data is collected in XYZ or ENU coordinates (i.e., the coordinate system relative to the probe head or the geophysical coordinate system, respectively).[10] Data with mild to moderate phase-wrapping is easily corrected, but extreme cases of phase-wrapping, such as encountered

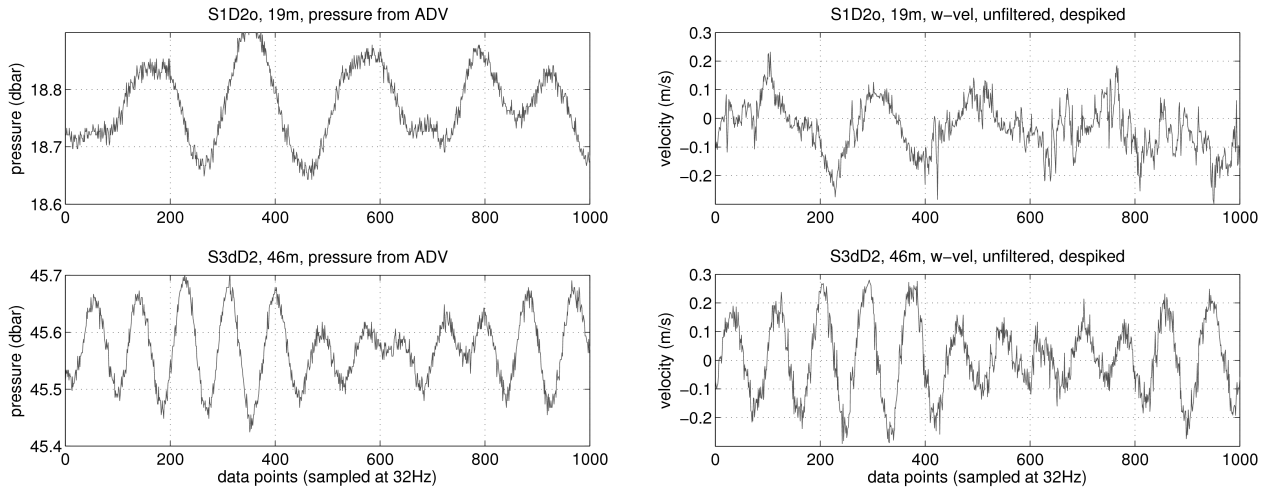

Figure 3. Pressure (left) and velocity (right) time series from the Florida coast (Station 1, top) and the Bahamas (Station 3d, bottom) illustrate platform motion felt by the ADV/CT probes on the iMast. The extent of vertical movement by the frame is similar at both stations, but the period of motion is shorter and the vertical velocities are higher at the Bahamas station. Meteorological conditions were recorded as calm at Station 1 (yet with strong currents and drift), and as rougher with pronounced swell at Station 3.

in our data, can be too noisy to unwrap successfully and may introduce spuriously high values for TKED dissipation. These data had to be rejected in our analysis. Generally, one should ensure that the ambiguity velocity is not exceeded during deployment. Note, however, that an increase in nominal velocity range, i.e., a decrease in pulse separation, will also cause a decrease in instrument resolution.

Another challenge when attempting to quantify TKED with measurements taken from a moving platform is the issue of platform motion. Surface waves, pitch and roll, and cable vibrations all may introduce motion that can spread through the ISR of the spectrum. The effect of surface waves and swell can be seen in our data in both the time series and spectra (Figures 3, 4). The unfiltered spectrum shown in the left panel of Figure 4 exhibits a peak in the high-frequency part of the ISR corresponding to the dominant period of the wave-like motion seen in the time series. This can be attributed to platform motion. This peak may be present in spectra from all three velocity components or may only be found or be more expressed in the vertical and transverse components. We apply a Chebyshev filter with minimal damping to the time series to reduce the effect of this motion on the spectra. The effect of this filter can be seen in the spectrum shown in Figure 4, right-hand panel. The filtering does not affect the overall value of the spectrum in the ISR, nor does it significantly damp the signal, it merely improves the spectral fit in the ISR.

2.2.2 Temperature Dissipation rate - TD

For the estimation of TD rates from the temperature time series, we followed Ref. 11, fitting temperature gradient spectra to the theoretical Batchelor spectrum. This technique involves fitting the temperature gradient spectra in the dissipative high-frequency range of the spectrum. To obtain temperature gradient spectra from the temperature time series, we again invoke Taylor's frozen turbulence hypothesis and use

$$\frac{dT}{dx} = \frac{1}{U}\frac{dT}{dt} \tag{3}$$

and $\hat{k} = f/U$ (note that $\hat{k}$ has units of cpm) . For isotropic turbulence, the dissipation rate of the temperature variance can be described as

$$\chi_T = 6D_T\langle\frac{dT}{dx}\frac{dT}{dx}\rangle = 6D_T\int_0^\infty \Psi_{T_x}(k)\,dk, \tag{4}$$

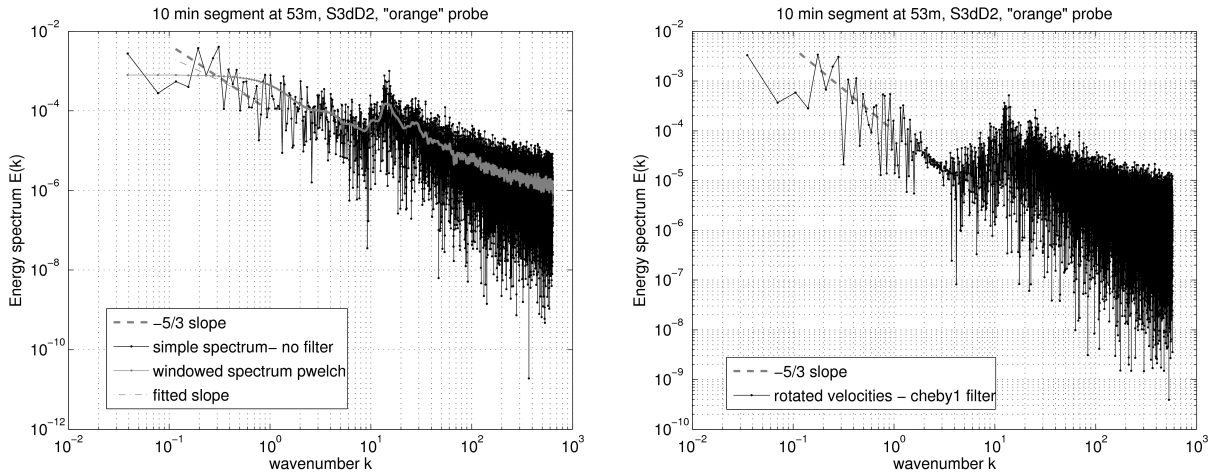

Figure 4. Energy spectra from the streamwise velocity component at Station 3 in the Bahamas (Tongue of the Ocean). Note the peak at wavenumber $k \approx 10 - 20 rad\, m^{-1}$ (corresponding to a period of about 2-5s) in the unfiltered spectra (left), which is due to ship/platform motion. For this spectrum, U was chosen to be the larger of the horizontal velocity components. The filtered spectrum is shown on the right. Here, the velocities were rotated into a new frame of reference with $\overline{U} = (\overline{U}_1, 0, 0)$. The slope in the inertial subrange of the spectra is in agreement with the Kolmogorov $-\frac{5}{3}$ law.

where D_T is the thermal diffusivity, and $\Psi_{T_x}(k)$ is the wavenumber spectrum of $\frac{dT}{dx}$, the alongpath component of the temperature gradient.[11] We then explored the use of MLE spectral fitting to our data.[9] However, since our spectra do not resolve the high-frequency part of the spectrum, up to the Batchelor cut-off wavenumber k_B, the method described by Ref. 11, which is based on integrating the theoretical spectrum, is more appropriate for our data. For consistency, the data are again filtered for platform motion, which does however not affect the frequency range of the spectrum involved in the Batchelor fit. Furthermore, a spectral correction to the signal measured by the thermistor is applied through a single pole response function

$$H^2(\hat{k}) = \frac{1}{[1 + (U\hat{k}/f_c)^2]}, \tag{5}$$

with $f_c = 20Hz$.[11,12] The correction is done by multiplying the spectra by the inverse of the filter function.

To ensure that U varies as little as possible over the segment used to calculate temperature gradient spectra, spectral estimates were done from 4-second data segments and the results for χ were averaged. Our sampling frequency of $32Hz$ is at least three to four times lower than that generally used to estimate χ from temperature measurements. Despite this shortcoming, which is due in part to the limitation of the temperature probe being integrated with and controlled by the ADV, we find the TD rates we obtain from either method to be robust. Here, we chose not to report an error associated with our estimate of χ, since uncertainties are introduced in a number of ways, which can not adequately be quantified at this point.

The Batchelor spectral fitting technique can also be applied to estimate ϵ, through the relationship

$$k_B = [\frac{\epsilon}{\nu\, D_T^2}]^{\frac{1}{4}}, \tag{6}$$

which ties the Batchelor wavenumber k_B to the TKED rate ϵ (ν is the molecular viscosity of water), as well as the relationship

$$\epsilon_\chi = \frac{N^2 \chi}{2\Gamma \langle \frac{dT}{dz} \rangle^2}, \tag{7}$$

where ϵ_χ signifies TKED derived from χ. Here, $\Gamma = 0.2$, N is the local buoyancy frequency, and $\langle \frac{dT}{dz} \rangle$, is the local temperature gradient, which can be estimated directly from our data following the procedure described

in Ref. 11. The mean temperature gradient $\langle \frac{dT}{dz} \rangle$ is estimated from $1min$ long data segments, either directly preceeding or following the $4s$ segment from which temperature gradient spectra were calculated. Likely due to the fact that our spectra are severely underresolved in the range preceeding k_B, as well as due to uncertainties associated with local estimates of $\langle \frac{dT}{dz} \rangle$ and N^2, we found our estimates of ϵ_χ from the temperature gradient spectra to be less robust than those of χ itself.

3. RESULTS

3.1 TKED

We compare data from two stations, Station 1 near the Florida coast, on the shelf in an area influenced by the Gulf Stream, and Station 3d in the Bahamas, in a deep basin called the Tongue of the Ocean (Fig. 1). Repeat casts from the VMP near Station 1 reveal an energetic environment in the upper ocean, with TKED rates ϵ reaching as high as $10^{-5}m^2s^{-3}$ in the top $20m$ above the thermocline and around 10^{-7} to $10^{-6}m^2s^{-3}$ in the thermocline (Fig. 5). The station was occupied for two days, June 30 and July 2, the VMP casts were taken on July 2. The differences in mixed layer depth and stratification between the two days can be explained by the temporal and spatial variability characteristic of this highly energetic area on the east Florida shelf, especially since the boat was drifting during deployments. The variability shown during successive VMP casts is also typical of such a deployment strategy, since the boat will drift in and out of turbulent patches, which in themselves are intermittent and vary in both space and time. The TKED rates from the ADV on the iMast fall well within the range predicted by the VMP measurements. The ADV data was clean enough for the estimation of ϵ near $20m$ depth from all three ADVs on both days,and the values center around $\epsilon \approx 10^{-6}m^2s^{-3}$. Excessive noise and phase-wrapping in several probes at deeper depths led to fragmented data that did either not resolve the ISR or exhibited unrealistically high values of ϵ due to noisy velocity series and had to be rejected. The data from which ϵ could be calculated for the deeper pauses, at around $27m$ depth on June 30 and near $43m$ depth on July 2 show that they fall within the range of values experienced by the VMP. The large margin of error at around $27m$ can also be attributed to high levels of noise and phase-wraps in the velocity data. The data from around $10m$ on June 30 show TKED values significantly lower that those of the VMP on July 2. This is not unexpected given the intermittent and spatially varying nature of turbulence, and can be explained by different wind conditions for the two days, affecting the mixing in the upper ocean, as well as spatial differences between locations of casts taken from the drifting vessel. Estimates of TKED from the microstructure temperature data, ϵ_χ also mostly fall within the range of ϵ predicted by the VMP and the ADVs on the iMast, but as explained in Section 2.2.2, they were considerably less robust than the values from the ADV.

The environment in the Tongue of the Ocean, a stretch of deep water in the central Bahamas, near the Berry Islands, is found to be considerably more quiescent than the energetic ambient on the east Florida shelf. TKED rates found with the VMP in this area on July 7 center around $\epsilon \approx 10^{-9}$ to $10^{-8}m^2s^{-3}$, with values reaching as high as $10^{-7}m^2s^{-3}$ in the thermocline and $10^{-6}m^2s^{-3}$ closer to the ocean surface (Figure 6). The values from the ADVs, where all pauses where taken around $50m$ depth, are higher than those of the VMP, and center around $10^{-6}m^2s^{-3}$. The estimates of ϵ_χ from the CT data also fall within this range. The data at this station was very noisy and phase-wrapping was strong, to the point where the ADV data from the repeat occupations of this station on July 6 and July 8 were unusable. Video frames from the camera on the iMast taken during deployments revealed vibrations of the frame and/or camera housing. These vibrations may be the cause of the strong noise and excessive phase-wrapping found in the data from this station. This may also have affected the data on July 7 from which ϵ was calculated, and may have led to the high bias in the results. An alternative and perhaps more likely explanation for the higher values from the ADVs at this depth and station, is that the frame on which the probes were mounted, being pulled through the water with vertical excursions of $\sim 30cm$ and vertical velocities up to $\sim 30cms^{-1}$ caused an increase in ambient turbulence levels in this quiescent environment (Figure 3). The effect of the frame on ambient turbulence levels may have been less noticeable in the more energetic waters on the Florida shelf. Additionally, weather conditions on the Florida shelf were calm, yet with strong drift currents, whereas conditions during the Tongue of the Ocean deployments were breezy with significant swell, which may have contributed to cable and frame motion.

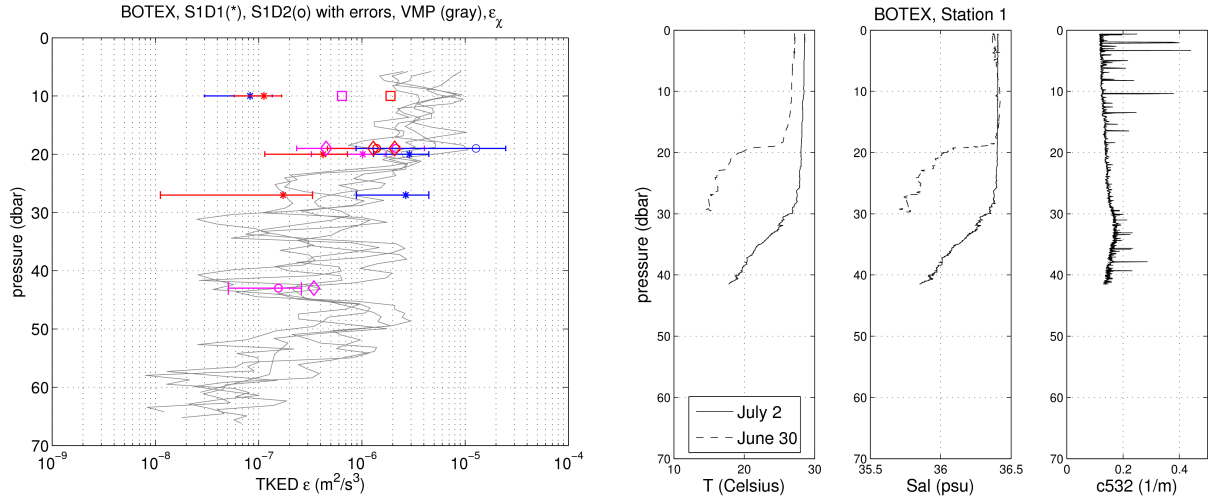

Figure 5. TKED rates from Station 1 on the Florida coast from VMP and Nortek ADV on the iMast (left). The station was occupied on June 30 and July 2, 2011. Stratification and c532 from the CTD/optics package at this station are shown on the right. The thin gray lines show different realizations of VMP drops for ϵ on July 2. Estimates of TKED rate ϵ from the ADV data are shown as stars (June 30) and circles (July 2) with associated error bars (2 standard errors estimated via MLE technique). Individual points signify data from three different instruments (color-coded red, purple and blue, in the electronic version of the paper). Diamonds (July 2) and squares (June 30) are estimates of ϵ_χ from temperature gradient spectra from the microstructure temperature probe on the iMast.

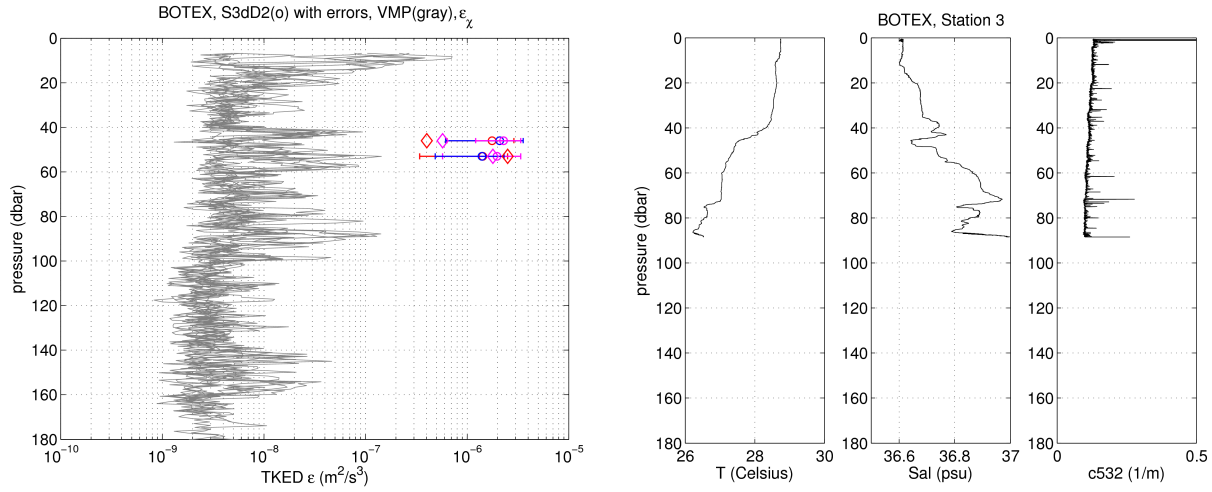

Figure 6. TKED rates from Station 3 (Bahamas, Tongue of the Ocean) from VMP and Nortek ADV on the iMast (left). Stratification and c532 from the CTD/optics package at this station are shown on the right. The thin gray lines show different realizations of VMP drops for ϵ. Estimates of TKED rate ϵ from the ADV data are shown as circles with associated error bars (2 standard errors estimated via MLE technique). Individual points signify data from three different instruments (color-coded red, purple and blue, in the electronic version of the paper). Diamonds are estimates of ϵ_χ from temperature gradient spectra from the microstructure temperature probe on the iMast.

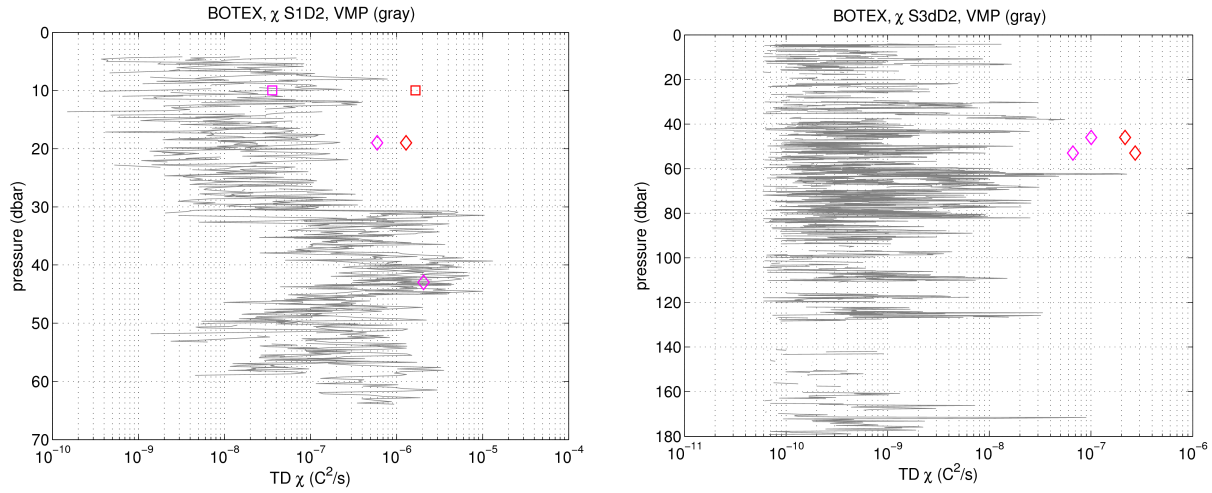

Figure 7. TD rates from Station 1 (FL coast) and Station 3 (Bahamas, Tongue of the Ocean) from VMP and temperature microstructure probe on the iMast. The thin gray lines show different realizations of the VMP drops, the diamonds (squares for S1 on June 30) are TD estimates from temperature gradient spectra from the microstructure temperature probe. Individual points signify data from two different instruments (color-coded red and purple, in the electronic version of the paper).

3.2 TD

Estimates of TD rates χ from the microstructure temperature probe on the iMast exhibit a similar pattern. The values largely fall within the range predicted by the VMP, except at the Bahamas station, and for the pause above the thermocline at the Florida station (Figure 7) . Especially at the Florida station, the TD rates from the VMP can be seen to show a significant increase in the thermocline, up to three orders of magnitude larger than in the well-mixed unstratified near-surface layer. The Tongue of the Ocean stations also exhibits an increase in TD near the thermocline, but it is less pronounced than at the Florida station, consistent with a much weaker thermocline near Station 3d. The values of χ from the CT data near the $20m$ pause in the Florida stations, which are slightly higher than those of the VMP, can be explained by the vessel drifting northwestward and onto the shelf into shallower water during deployment. The iMast data at Station 1 was taken after the VMP casts, and the drift direction of the vessel onto the narrow shelf would have led the probes to sample through an area right above the shoaling thermocline, showing increased temperature dissipation.

The estimates of χ in the Bahamas from the iMast data at around $50m$ depth also show values near or above the upper bound of those seen by the VMP. The time series were taken right above the thermocline in this area, and here, swell-induced vertical motion of the frame across layers of increased TD, or even mixing induced by the frame itself, could certainly have contributed to the slight high bias in the χ estimates. However, instrument vibration and noise contamination can not be completely ruled out and may also have affected the estimates of χ at this station, especially since high-frequency noise was visible in these temperature time series. Nonetheless, note that the χ estimates from the microstructure temperature data in the Tongue of the Ocean, which were taken just above the thermocline, center around $10^{-7}C^2s^{-1}$, about an order of magnitude smaller than those above or near the thermocline at the Florida station, consistent with the difference in turbulence levels seen at the two stations.

3.3 Effect on optics - Sn

The effect on the optical transfer function can be described as a function of TKED and TD, $S_n \sim \chi\epsilon^{-\frac{1}{3}}$.[13] S_n is related to light attenuation by optical turbulence as a function of microstructure and spatial frequency range. We estimate values of S_n for Stations 1 and 3d, in Florida and the Bahamas, respectively, for the pauses near or just above the thermocline, where we can expect the strongest optical turbulence. The units are contained within a proportionality constant and we neglect them in the following estimate. At Station 1

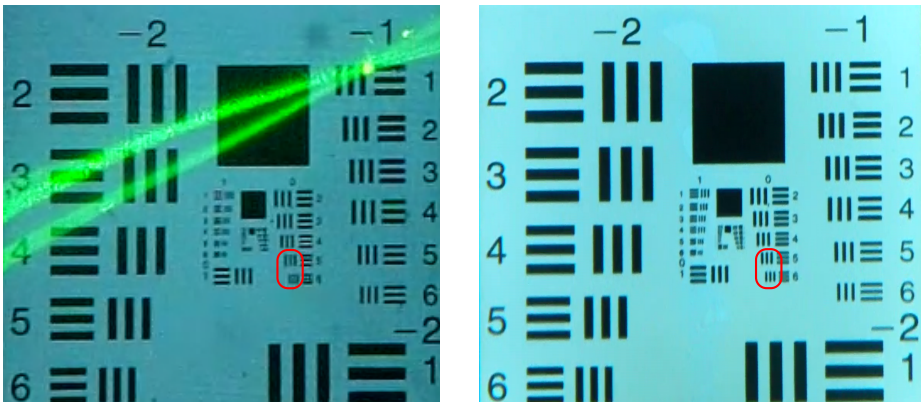

Figure 8. Still frames from video taken on iMast near the Florida coast (S1, left) and in the Bahamas (S3, right). Red rectangles indicate high-frequency parts of the image, which, qualitatively, appear more blurred in the image from the Florida coast, consistent with degradation by optical turbulence. Also note the green light beam across the image to the left, indicating backscatter from particles in the water.

near the Florida coast, at $\sim 20m$ depth, with a beam attenuation at $532nm$ of $c532 \approx 0.15m^{-1}$, the value becomes $S_n \sim 10^{-7}C^2s^{-1}(10^{-6}m^2s^{-3})^{-\frac{1}{3}} \approx 10^{-5}$ with the VMP data, or $S_n \sim 10^{-6}C^2s^{-1}(10^{-6}m^2s^{-3})^{-\frac{1}{3}} \approx 10^{-4}$ from ADV/CT data on the iMast. In the Bahamas, near $50m$ depth and with a $c532 \sim 0.1m^{-1}$, $S_n \sim 10^{-9}C^2s^{-1}(10^{-8}m^2s^{-3})^{-\frac{1}{3}} \approx 5 \times 10^{-7}$ from the VMP and $S_n \sim 10^{-7}C^2s^{-1}(10^{-6}m^2s^{-3})^{-\frac{1}{3}} \approx 10^{-5}$ from the iMast. The effect of optical turbulence is thus predicted to be more pronounced in the more energetic environment near the Florida coast than in the deeper waters in the Tongue of the Ocean. Frames taken from the videos on the iMast qualitatively confirm this finding (Figure 8). At the same level of magnification, the image from the Bahamas stations appears clearer, especially at high frequencies, than the image from the Florida station, for similar levels of particle concentrations.

4. SUMMARY AND DISCUSSION

We collected high-resolution velocity and temperature data along with high-speed video frames in the waters off the Florida coast and the Bahamas to investigate optical turbulence. A VMP was deployed to collect profiles of velocity shear and temperature gradient data for comparison with the data collected on the iMast. TKED and TD rates were inferred from the ADV and temperature microstructure data, compared to the dissipation rates from the VMP and put into the context of optical turbulence.

The estimates of TKED and TD from the ADV and temperature microstructure data fall largely within the range of turbulence levels observed with the VMP. Temporal and spatial variability in oceanic turbulence, which is well-known to be intermittent and "patchy", also affect the match between VMP and ADV/CT data. The most pronounced differences can be explained by the deployement strategies, i.e. drift across a shoaling thermocline on the Florida shelf, and possibly frame-induced turbulence in the Bahamas. Overall, the data from ADV and temperature microstructure probe are able to adequately describe the turbulence levels experienced by the iMast, deployed for the investigation of optical turbulence. However, noise from platform motion and vibrations, apparent in both velocity and temperature data, can complicate the estimation of TKED and TD from the ADV/CT and complemetary measurements with a dedicated turbulence instrument, such as the VMP, are an invaluable tool to aid in data analysis and guide error estimates.

Increased levels of optical turbulence are expected to be found above or near the thermocline. Optical turbulence levels predicted by the VMP and ADV/CT data at the two stations are confirmed qualitatively by video frames taken during the iMast deployments.

This study was the first comprehensive effort comparing a traditional profiling approach for measuring turbulence to estimates of dissipation rates from an ADV/CT package on a moving platform for the investigation of optical turbulence in the ocean. Such a comparison is challenging but necessary for efforts aimed at quantifying oceanic microstructure in the context of studying EO signal transmission. The results of this work will help us

address sampling challenges for future deployments of iMast to study optical turbulence and are useful for an improved understanding of the use of ADVs to probe oceanic turbulence. Measuring turbulence in the ocean has long been known to be a challenging task, and further studies of optical turbulence will benefit from being conducted in a controlled laboratory environment. Such laboratory experiments, complemented by numerical simulations, are underway and, along with the results from present and future field measurements, will help shed light on the processes involved in optical turbulence in the ocean.

ACKNOWLEDGMENTS

We would like to thank Drs. Danielle Wain, Cynthia Bluteau and Barry Ruddick for sharing their respective Matlab scripts for the calculation of TKED and TD rates, parts of which we incorporated in our own processing routines. The captain and crew of the R/V Walton Smith are gratefully acknowledged. We thank Dr. Clare Reimers and UNOLS for awarding S. Matt participation in the 2012 UNOLS training cruise and for helpful discussions, which directly benefited the analysis of the data presented here. This work was supported by ONR/NRL 73-6604. Silvia Matt is supported by a National Research Council Research Associateship.

REFERENCES

[1] Hou, W., Woods, S., Jarosz, E., Goode, W., and Weidemann, A., "Optical turbulence on underwater image degradation in natural environments," *Appl. Opt* **51**(15) (2012).

[2] Hou, W., Jarosz, E., and Woods, S., "Bahamas optical turbulence exercise (BOTEX)," *Proc. SPIE* **8372** (2012).

[3] Wolk, F., Yamazaki, H., Seuront, L., and Lueck, R. G., "A new free-fall profiler for measuring biophysical microstructure," *J. Atmos. Oceanic Technol.* **19**, 780–793 (2002).

[4] Oakey, N. S., "Determination of the rate of dissipation of turbulent energy from simultaneous temperature and velocity shear microstructure measurements," *J. Phys. Oceanogr.* **12**, 256–271 (1982).

[5] Bluteau, C. E., Jones, N. L., and Ivey, G. N., "Estimating turbulent kinetic energy dissipation using the inertial subrange method in environmental flows," *Limnol. Oceanogr. Methods* **9**, 302–321 (2011).

[6] Lesieur, M., [*Turbulence in Fluids, 4th Edition*], Springer (2008).

[7] Tennekes, H. and L.Lumley, J., [*A first course in turbulence*], MIT Press (1972).

[8] Rusello, P. and Cowen, E., "Turbulent dissipation estimates from pulse coherent doppler instruments," in [*Current, Waves and Turbulence Measurements (CWTM), 2011 IEEE/OES 10th*], 167–172 (2011).

[9] Ruddick, B., Anis, A., and Thompson, K., "Maximum likelihood spectral fitting: The batchelor spectrum," *J. Atmos. Oceanic Technol.* **17**, 1541–1555 (2000).

[10] Rusello, P. J., "A practical primer for pulse coherent instruments," *Nortek Technical Note* **TN-027** (2009).

[11] Moum, J. and Nash, J., "Mixing measurements on an equatorial ocean mooring," *J. Atmos. Oceanic Technol.* **26**, 317–336 (2009).

[12] Bogucki, D. J., H.Luo, and Domaradzki, J. A., "Experimental evidence of the kraichnan scalar spectrum at high reynolds numbers," *J. Phys. Oceanogr.* **42**, 1717–1728 (2012).

[13] Hou, W., "A simple underwater imaging model," *Optics Letters* **34**(17) (2009).